Temperature dependence of ministop band in double-slots photonic crystal waveguides

Kaiyu Cui,[a] Yidong Huang,[b] Gengyan Zhang, Yongzhuo Li, Xuan Tang, Xiaoyu Mao, Qiang Zhao, Wei Zhang, and Jiangde Peng
Department of Electronic Engineering, State Key Laboratory of Integrated Optoelectronics, Tsinghua University, Beijing 100084, People's Republic of China

(Received 15 September 2009; accepted 12 October 2009; published online 10 November 2009)

We proposed and fabricated a double-slots photonic crystal waveguides (PCWGs) structure formed by introducing two slots into PCWGs with air-bridge structure on silicon-on-insulator substrate. The mode characteristics of double-slots PCWGs were investigated theoretically and experimentally. The transmission spectra present a sharp and deep dip (22 dB with bandwidth of 6 nm) caused by ministop band in the proposed structure, which is 15 dB deeper than that in the W3 PCWG. Additionally, dependence of the dip on temperature in the double-slots PCWG was measured and a temperature coefficient 0.159 nm/°C can be concluded. © *2009 American Institute of Physics*. [doi:10.1063/1.3258072]

Photonic crystal (PC) slabs with two-dimensional (2D) PC structures located within high index contrast slabs, have attracted a lot of attention[1–4] because of the combining light-wave confinement mechanism of in-plane photonic band gap (PBG) and vertical total internal reflection, as well as their easy fabrication processes compared to three-dimensional PC. By introducing line defects into the PC slabs, the defect modes would appear in the PBG and PC waveguides (PCWGs) can be formed. Mode coupling between the defect modes in PCWGs could transfer the energy from the fundamental guided mode to the high-order modes which propagate backward with large losses. Therefore, in the frequency region of the fundamental mode, minigaps, so called ministop band (MSB),[5] would appear and MSB-dips can be observed in the transmission spectra. S. Oliver and H. Benisty's group and T. F. Krauss's group have given many valuable theoretical and experimental studies about MSB.[5–10] Transmission spectra of MSB have been measured by internal light source technique for waveguides in GaAs and InP-based PC heterostructures which correspond to weak index confinement structures in the vertical direction.[5,6,11] Because mode coupling is the basic mechanism for many functional PCWGs devices, such as filters, splitters, switches, etc., the mode coupling in just one PCWG provides a simple platform for compact device. Thus, many promising applications based on MSB have been proposed, such as optical gain enhancement,[7,12] slow light,[13] fluid sensor,[14] mode selective mirror,[9] and spectral filter.[10,11]

However, MSB is generally formed in multimode PCWGs[5,6,11,13] and the interaction of these multimodes will degrade the transmission performance.[15] Additionally, effective adjustment of MSB is not feasible. In this paper, we proposed a structure by inducing double slots into traditional PCWGs to control MSB by adjusting the defect modes in the PBG and their coupling strength. Theoretical and experimental results show that the transmission spectra of proposed double-slots PCWGs present sharp and deep MSB-dip compared to that of the traditional PCWGs. The sharp and deep MSB-dip means better filter and mode selective characteristics, and also benefits for the applications of slow light, optical gain enhancement, and fluid sensor. This MSB-dip can be controlled by not only the structural parameters, such as the position and width of the slots but also the temperature. The temperature coefficient of the MSB-dip wavelength, $\Delta\lambda/\Delta T=0.159$ nm/°C, can be concluded from the experiment results.

Structure of the double-slots PCWG is shown in Fig. 1. The lattice period and the radius of the PC holes are denoted as a and r, respectively. Here, W3 PCWG was selected to induce the double slots, because MSB in W3 PCWG has been extensively studied both in mechanism and experiment.[5,6,11,13] Two slots are symmetrical in the PCWG, where W_{slot} and W_0 represent the width of the slot and the central waveguide, respectively. Silicon on insulator (SOI) with air bridge structure was used to fabricate the proposed structure. We calculated the band structure in ΓK direction by 2D plane wave expansion method (PWE) with an effective refractive index[16] $n_{eff}=2.67$ in the vertical direction. The n_{eff} was determined by the thickness of the fabricated PC slab and the vertical index distribution. The validity of $n_{eff}=2.67$ for our fabricated samples can be further confirmed by the experiment results of transmission spectra, which fitted well with the simulation results of 2D PWE and 2D finite-difference time-domain method (FDTD). Figure 2 shows the calculated transverse electric mode band structures of W3 and double-slots PCWGs, respectively, at the same $r/a=0.28$, where $W_0=1.2a$, and $W_{slot}=0.2a$ for the double-slots PCWG. The order of the defect modes was labeled in the band gap according to the number of zero crossings of its magnetic field distribution.

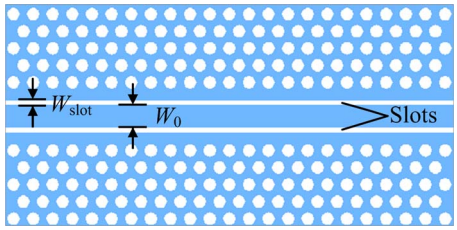

FIG. 1. (Color online) Structure of the double-slots PCWG which is formed by inducing double slots into a W3 PCWG.

[a]Electronic mail: cuiky05@mails.tsinghua.edu.cn.
[b]Electronic mail: yidonghuang@tsinghua.edu.cn.

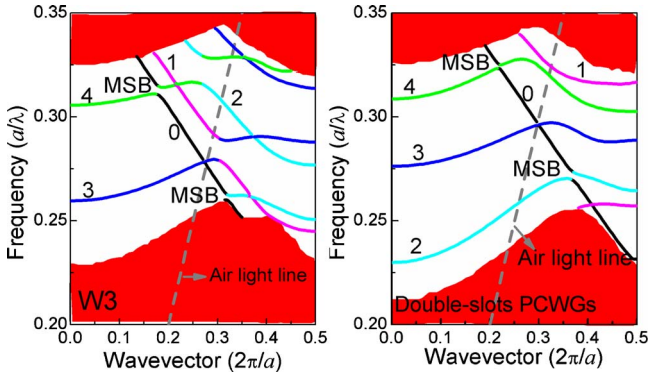

FIG. 2. (Color online) TE mode band structure of (a) W3 PCWG with $r/a=0.28$, (b) double-slots PCWG with $r/a=0.28$, $W_0=1.2a$, and $W_{slot}=0.2a$.

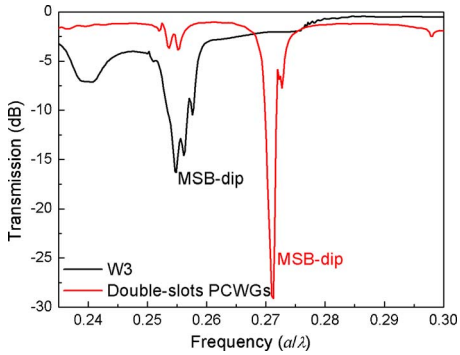

FIG. 3. (Color online) Transmission spectra simulated by FDTD for W3 and double-slots PCWGs ($W_0=1.2a$, and $W_{slot}=0.2a$) with same $r/a=0.28$.

It can be seen from Fig. 2 that there are two MSBs for the fundamental mode for both W3 and double-slots PCWGs. One is above the air light line and the other is below the air light line. Because modes above the air light line will cause huge vertical radiation loss,[4] we just discuss MSB below the air light line, here. In W3 PCWG, MSB is caused by the coupling between the fundamental mode and the band edge mode, which has larger transmission loss than that of the defect mode. Additionally, there are many coupling modes, such as 1st and 3rd modes, 2nd and 4th modes, in W3 PCWG and the complex coupling modes will degrade the MSB transmission performance. In the double-slots PCWG shown in Fig. 2(b), the MSB is formed by coupling between the fundamental mode and the 2nd order mode and lies below the air light line, which can be guided better than that in W3 PCWG because of the less loss. On the other hand, the defect modes in PBG of the double-slots PCWG are effectively adjusted and the defect modes around the frequency of MSB are removed which is beneficial to transmission performance. In addition, two slots weak the coupling between the fundamental mode and the 2nd order mode. This is promising to obtain a narrow MSB-dip, which can be explained by the coupled-mode theory.[6] The MSB bandwidth in the lossless case can be given[6,11]

$$\Delta = \frac{a}{2\pi}\frac{4\kappa}{n_+ + n_-}. \tag{1}$$

Here, Δ is the MSB bandwidth, κ is the coupling coefficient, n_+ and n_- are the phase refractive index of the forward-propagating and backward-propagating waves. Due to the fact that the fundamental mode in the double-slots PCWGs is mainly determined by the central waveguide (between two slots with width of W_0 shown in Fig. 1), the coupling intensity between the forward index-guided and backward crystal-guided propagating modes[11] is smaller than that of W3 PCWG caused by the separation of the two slots, namely a small κ for the double-slots PCWG. Therefore, a narrow dip can be expected in the double-slots PCWG, and effective control of the MSB bandwidth and frequency is feasible in this structure by changing the position and width of slots.

Transmission characteristics were simulated by 2D FDTD method for the two types of PCWGs. Results are shown in Fig. 3. It can be seen that MSB-dip in the double-slots PCWG is rather sharp and deep compared to that in the W3 PCWG.

We fabricated both proposed double-slots PCWGs and traditional W3 PCWGs on SOI substrate with air-bridge structure. The scanning electron microscope (SEM) images are shown in Fig. 4.

The SOI wafer has a 200-nm-thick silicon slab on the top of a 3-μm-thick SiO_2 layer. Using ZEP-520A as a resist mask, pattern for PCWGs with the input and output stripe waveguides was generated by electron beam lithography. Then inductively coupled plasma dry etching using CF_4 and Ar mixture was employed to transfer the pattern to the silicon slab. After removing the resist mask, a 600-nm-thick SiO_2 cladding layer was deposited on the surface, which would help to protect the input and output waveguides in the air-bridge etching process and improve the coupling efficiency. Following this, photolithography was used to create an opening just on the PCWGs region for forming the air-bridge structure by wet etching. Buffer hydrofluoric acid was used to etch the underlying SiO_2 within the wet-etching opening area, so that the air-bridge structure was formed. Finally, we removed the photoresist and ground the wafer to the thickness about 100 μm, and cleaved it into about 1-mm-long samples for measurement.

The structure parameters for the double-slots PCWG are $a=420$ nm, $r=120$ nm, $W_{slot}=90$ nm, $W_0=500$ nm, and the length for double-slots PCWGs L is $50a$ ($L=21$ μm); the structure parameters for the W3 PCWG are $a=390$ nm, $r=110$ nm, and the length for W3 PCWGs is also $50a$ ($L=19.5$ μm). It should be noticed in Fig. 4(a) that we designed the slots termination to extend outside of the hole edge boundary to improve the coupling efficiencies, following the reported optimized deign in Ref. 8.

The transmission spectra of these samples were measured with an autocoupling alignment system. The measurement system included a light source, a polarization controller, an input tapered polarization-maintaining lens fiber, a precise fiber alignment system, an output tapered lens fiber, a power meter, and a monitor. The light source was a tunable laser with wavelength tuning range from 1350 to 1630nm.

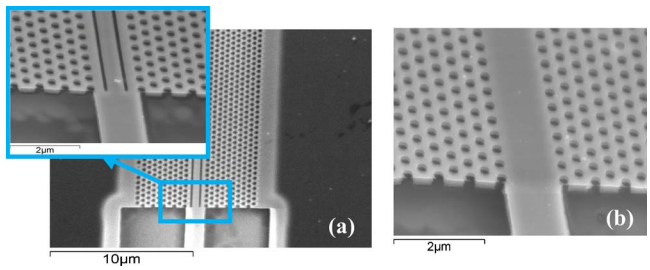

FIG. 4. (Color online) SEM images for (a) double-slots PCWGs and (b) W3 PCWGs.

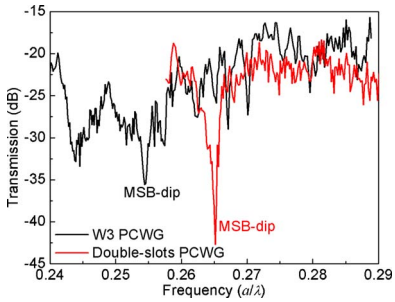

FIG. 5. (Color online) Transmission spectra of W3 and double-slots PCWGs with a length of 50 lattice constants ($L=50a$).

The polarization state of the tunable laser was determined by a special polarization controller. The precise autocoupling fiber alignment system can be controlled by a computer via a general purpose interface bus card and the accuracy of this system is about 5 nm. The output of the tested sample was coupled to the output tapered lens fiber and measured by the power meter.

Figure 5 shows the transmission spectra of the W3 and double-slots PCWGs, both with lengths of $L=50a$. The shape and position of the MSB-dips are in good agreement with the theoretical predictions. The MSB-dip in double-slots PCWGs is much sharper and narrower than that in the W3 PCWG, which has a 22 dB transmitted power extinction ratio and a bandwidth of 6nm with the fabricated parameters.

Besides the narrow bandwidth, the MSB-dip is much deeper than that of W3 PCWGs with the same length $L=50a$, namely the extinction ratio of W3 PCWGs is worse than that of double-slots PCWGs. This is because of larger losses in W3 PCWGs caused by the interaction between band edge mode and multimode. A high extinction ratio of 22 dB can be obtained from the double-slots PCWG with a length of only 21 μm.

Additionally, temperature dependence of the MSB-dip was measured for the double-slots PCWG. The measurement results are presented in Fig. 6. It can be seen that the MSB-dip moves to low frequency (redshift in wavelength) with temperature increasing. This is because the refractive index of the silicon slab increases when temperature grows. The temperature coefficient $\Delta\lambda/\Delta T=0.159$ nm/°C can be concluded from the experimental results shown in Fig. 6(b), where the frequency at half maximum (along the position of the arrow) changes with different temperatures. This result shows the potential applications of double-slots PCWGs as modulators and optical switchers based on the thermal-optical adjustment.

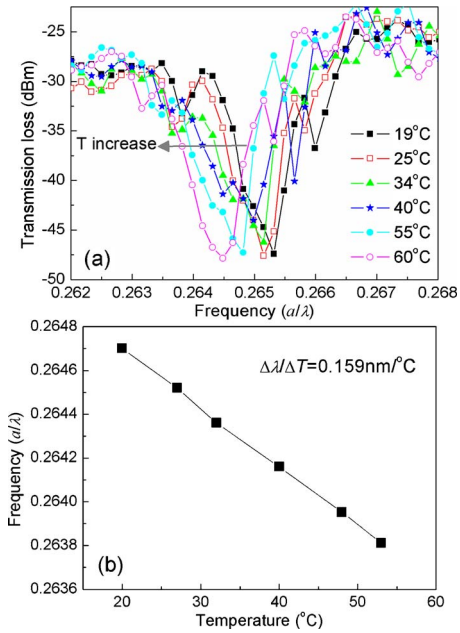

FIG. 6. (Color online) (a) Transmission spectra of double-slots PCWGs at different temperature. (b) Frequency at half maximum (along the arrow) moves with temperature.

In conclusion, we have presented a double-slots PCWGs structure by introducing two slots in PCWGs. Defect modes near MSB can be effectively adjusted, which will improve the performance of devices based on MSB effect significantly. Double-slots PCWGs and traditional W3 PCWGs on SOI substrate with air-bridge structure were fabricated and the transmission spectra were measured and compared. A narrow, sharp, and deep MSB-dip in the transmission spectra was obtained for double-slots PCWGs with 22dB transmitted power extinction ratio and bandwidth of 6 nm from a short PCWGs length (~21 μm). This agrees well with the theoretical prediction for weak coupling intensity caused by the double slots. Additionally, dependence of dips on temperature was measured and the temperature coefficient $\Delta\lambda/\Delta T=0.159$ nm/°C can be concluded. Based on the theoretical and experimental analysis, double-slots PCWGs shows more promising applications than W3 PCWGs based on MSB effect.

This work was supported by the National Natural Science Foundation of China (NSFC-60537010), and the National Basic Research Program of China (973 Program) under Contract No. 2007CB307004.

[1]S. G. Johnson, S. H. Fan, P. R. Villeneuve, J. D. Joannopoulos, and L. A. Kolodziejski, Phys. Rev. B **60**, 5751 (1999).
[2]E. Chow, S. Y. Lin, S. G. Johnson, P. R. Villeneuve, J. D. Hoannopoulos, J. R. Wendt, G. A. Vawter, W. Zubrzycki, H. Hou, and A. Alleman, Nature (London) **407**, 983 (2000).
[3]S. G. Johnson, P. R. Villeneuve, S. H. Fan, and J. D. Joannopoulos, Phys. Rev. B **62**, 8212 (2000).
[4]M. Notomi, A. Shinya, S. Mitsugi, E. Kuramochi, and H. Y. Ryu, Opt. Express **12**, 1551 (2004).
[5]S. Olivier, M. Rattier, H. Benisty, C. Weisbuch, C. J. Smith, R. R. De, T. F. Krauss, U. Oesterle, and R. Houdre, Phys. Rev. B **63**, 113311 (2001).
[6]S. Olivier, H. Benisty, C. Weisbuch, C. Smith, T. Krauss, and R. Houdre, Opt. Express **11**, 1490 (2003).
[7]E. Schwoob, H. Benisty, C. Weisbuch, C. Cuisin, E. Derouin, O. Drisse, G. H. Duan, L. Legouezigou, O. Legouezigou, and F. Pommereau, Opt. Express **12**, 1569 (2004).
[8]A. Di Falco, L. O'Faolain, and T. F. Krauss, Appl. Phys. Lett. **92**, 083501 (2008).
[9]S. A. Moore, L. O'Faolain, T. P. White, and T. F. Krauss, Opt. Express **16**, 1365 (2008).
[10]M. Ayre, C. Cambournac, O. Khayam, H. Benisty, T. Stomeo, and T. F. Krauss, Photonics Nanostruct. Fundam. Appl. **6**, 19 (2008).
[11]M. Davano, A. Xing, J. W. Raring, E. L. Hu, and D. J. Blumenthal, IEEE J. Quantum Electron. **12**, 1164 (2006).
[12]K. Y. Cui, Y. D. Huang, W. Zhang, and J. D. Peng, J. Lightwave Technol. **26**, 1492 (2008).
[13]M. Davanco, A. M. Xing, J. Raring, E. L. Hu, and D. J. Blumenthal, Opt. Express **13**, 4931 (2005).
[14]L. Cao, Y. D. Huang, X. Y. Mao, F. Li, W. Zhang, and J. D. Peng, Chin. Phys. Lett. **25**, 2101 (2008).
[15]S. Mazoyer, J. P. Hugonin, and P. Lalanne, Phys. Rev. Lett. **103**, 063903 (2009).
[16]M. Qiu, Appl. Phys. Lett. **81**, 1163 (2002).